

Matrix Correction in X-Ray Fluorescence Analysis by the Effective Coefficient Method

Norbert Broll

Siemens AG, Automatisierungstechnik, P.O.B. 21 12 62, W-7500 Karlsruhe 21, Germany

Pierre Caussin

SOCABIM SA, 9 bis, villa du Bel-Air, F-75012 Paris, France

Markus Peter

Siemens AG, Automatisierungstechnik, P.O.B. 21 12 62, W-7500 Karlsruhe 21, Germany

Up till now, the well known effective coefficient method was used by referring to a single standard. The SFP (Siemens fundamental parameter) program additionally allows this method to be employed with several standards and to analyse samples containing an element that is not analysed. A modified algorithm, called the trace model, yields an improvement in the precision of the trace element analysis. The different variants are illustrated by practical applications.

INTRODUCTION

The first method for matrix correction in x-ray fluorescence analysis, based on the calculation of primary and secondary fluorescence, was introduced in 1968 by Criss and Birks,¹ who called it the fundamental parameter method. This method refines the concentrations iteratively until an acceptable agreement between calculated and measured intensities is found. For a long time, this procedure was limited by the capacity of computers and the accuracy of knowledge of fundamental parameters. Because of these difficulties, the method gave acceptable results only when the sample excitation was monochromatic.

After 1977, several methods²⁻⁴ were described which combined the theoretical calculation of the expected x-ray intensities for a standard or for a hypothetical sample with a semi-empirical algorithm of the Lachance-Traill,⁵ Claisse-Quintin⁶ or Lachance⁷ type. The influence coefficients obtained from these methods are approximations and not exact data. The same statement applies to the approach of De Jongh,⁸ where the influence coefficients are calculated by expansion in a Taylor series for the approximate composition of the standard.

In 1983, the fundamental or effective coefficient method⁹ was described. In this approach, for any given composition, the effective coefficients are directly derived from primary and second fluorescence.¹⁰ Instead of relative intensities R_i , which are often measured with difficulty, Broll and Tertian⁹ proposed an algorithm in order to compare the unknown sample with a standard sample. This procedure compensates for uncertainties in fundamental parameters and instrumental factors.

Later, Rousseau¹¹ proposed a method which in a first step estimates the composition of an unknown sample using a semi-empirical algorithm of the Claisse-Quintin

type. Fundamental coefficients¹² are then calculated. This calculation is more complicated than the approach using Tertian's identities,¹⁰ because for each pair of elements i, j , two coefficients α'_{ij} and h_{ij} , are introduced, instead of a single one, α_{ij} , as in Tertian's equations.

CURRENT STATUS OF THE FUNDAMENTAL PARAMETER METHODS

Mass absorption coefficients

Papers published recently^{13,14} did not improve the quality of data to any extent. Therefore, the tables of Leroux and Thin¹⁵ are still used, although it is known that errors of 5-30% for the mass absorption coefficients between the absorption edges belonging to the same series are possible. For a better knowledge of mass absorption coefficients, more intensive research¹⁶ is required.

Furthermore, semi-quantitative measurements, which include the analysis of very heavy and very light elements, require tables with extended ranges of wavelengths.

Excitation factors

In spite of some recent publications,¹⁷⁻²² the excitation factors E_i , which are the product of the probability of the ionization of an atom, the fluorescence yield and the probability of emission of the characteristic lines, are not better known. The estimated values reported in Table 1 for the very light elements ($K\alpha$ radiation) can be taken from various publications, although a considerable uncertainty has to be taken into account. Similar to the case for the excitation factors of the x-rays

Table 1. Excitation factors, $E_{K\alpha}$

Element	Z	$E_{K\alpha}$
Be	4	0.0005
B	5	0.0010
C	6	0.0022
N	7	0.004
O	8	0.007
F	9	0.010
Ne	10	0.013

derived from the K-series of the light elements, the factors for the L- and M-series are not well known either.

Spectral intensity distributions from x-ray tubes

In an attempt to estimate the spectral distribution of x-ray tubes, we did not use any theoretical calculations such as the Boltzmann electron transport equations.^{23,24} Instead, we worked with the spectral distributions experimentally determined with a Si(Li) detector using the method of Loomis and Keith.²⁵ Figure 1 shows the corrected spectral distribution of the continuum of an end-window x-ray tube with a rhodium target and a beryllium window of 125 μm thickness (Siemens AG66 type) at 50 kV excitation. The characteristic L, $K\alpha$ and $K\beta$ lines of the rhodium target contain 37.7, 4.7 and 0.9% of the total intensity (target lines plus continuous spectrum). The spectral distribution of the continuum can also be introduced into the programs in a semi-empirical manner. Fitting the equation

$$N(\lambda) \propto \left(\frac{\lambda}{\lambda_0} - 1\right)^q \frac{1}{\lambda^2} \exp(-Q' \mu_{\lambda}^n) \exp(-\mu_{\text{Be}, \lambda} \rho_{\text{Be}} d) \quad (1)$$

proposed by Tertian and Broll²⁹ to the experimental curve shown in Fig. 1, the following parameters are obtained: $q = 1.431$, $n = 0.8$ and $Q' = 0.0035$. The spectrum with these parameters is shown in Fig. 2 as a function of wavelength.

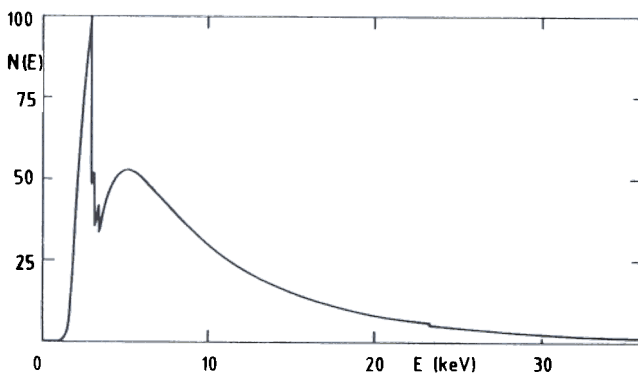


Figure 1. Spectral intensity distribution of the continuum of an end-window x-ray tube as a function of energy. Rh target, 50-kV excitation.

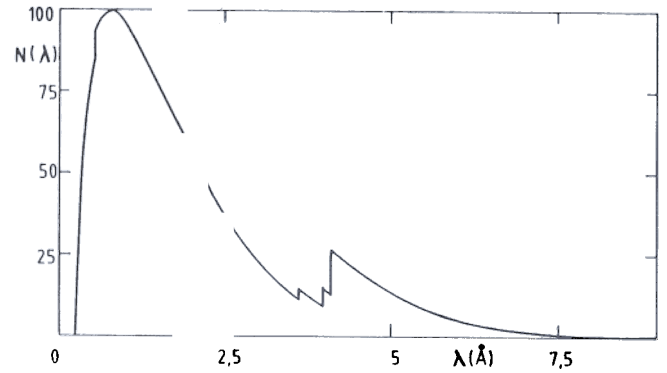


Figure 2. Spectral intensity distribution of the continuum of the Rh end-window x-ray tube as a function of wavelength.

Geometric factor

The exact knowledge of the geometric factor A (see Table 3) is very important, since it strongly affects the primary influence coefficients.³³ Different methods³⁴⁻³⁶ to determine the factor A were tried, e.g. one based on the method of effective coefficients and another comparing binary coefficients. It seems that the best results are obtained by a simple method, considering the Compton radiation.³⁷ The following values are obtained for the sample incidence angle ψ_1 and the sample take-off angle ψ_2 of the Siemens SRS 303 spectrometer: $\psi_1 = 60^\circ$ and $\psi_2 = 45^\circ$ (for the Siemens SRS 200 spectrometer the angles are $\psi_1 = 57^\circ$ and $\psi_2 = 45^\circ$).

BASIC EQUATION, TERTIAN'S IDENTITIES

The effective influence coefficients α_{ij} satisfying the Lachance-Trail equation can be calculated using Tertian's identities:¹⁰

$$\alpha_{ij} = \alpha'_{ij} - h_{ij} \frac{C_i}{R_i} \quad (2)$$

where α'_{ij} is the influence coefficient assigned to the primary fluorescence for i , h_{ij} is a factor due to secondary fluorescence ($h_{ij} C_j$ represents the fluorescence increment due to the secondary fluorescence intensity), C_i represents the concentration of the element i and R_i is the relative fluorescence intensity:

$$R_i = \frac{P_i + S_i}{P_{i,1}}$$

with

$$S_i = \sum_{j \neq i} S_{ij}$$

where j are the enhancing elements and

$$S_{ij} = P_i h_{ij} C_j$$

Table 2 shows the intensity relationships for the primary fluorescence P_i , the secondary fluorescence S_{ij} and the fluorescence of a pure element $P_{i,1}$. Table 3 defines the symbols used.

For the calculation of the effective influence coeffi-

Table 2. Basic equations

Intensity of primary fluorescence:

$$P_i = qE_i C_i \int_{\lambda_0}^{\lambda_{\text{abs},i}} \frac{\mu_{i,\lambda} I_\lambda d\lambda}{\mu_{s,\lambda} + A\mu_{i,\lambda}}$$

Intensity of secondary fluorescence:

$$S_{ij} = \frac{1}{2} qE_j C_j \int_{\lambda_0}^{\lambda_{\text{abs},i}} E_i C_i \mu_{i,\lambda} L \frac{\mu_{j,\lambda} I_\lambda d\lambda}{\mu_{s,\lambda} + A\mu_{s,\lambda}}$$

where

$$L = \frac{\ln\left(1 + \frac{\mu_{s,\lambda}/\sin\psi_1}{\mu_{s,\lambda_i}}\right)}{\mu_{s,\lambda}/\sin\psi_1} + \frac{\ln\left(1 + \frac{\mu_{s,\lambda}/\sin\psi_2}{\mu_{s,\lambda_i}}\right)}{\mu_{s,\lambda_i}/\sin\psi_2}$$

Intensity of fluorescence for a pure element:

$$P_{i,1} = qE_i \int_{\lambda_0}^{\lambda_{\text{abs},i}} \frac{\mu_{i,\lambda} I_\lambda d\lambda}{\mu_{i,\lambda} + A\mu_{i,\lambda}}$$

coefficients, initially the theoretical relative intensities are calculated according to

$$R_i = \frac{P_i + S_i}{P_{i,1}} = \frac{P_i}{P_{i,1}} (1 + h_{ij} C_j + h_{ik} C_k + \dots)$$

The values of the factors h_{ij} , h_{ik} , ..., are inherently determined during this calculation.

In the next step, the effective coefficients for the primary fluorescence α'_{ij} , α'_{ik} , ..., are derived by dividing the continuous spectrum of the x-ray tube into N monochromatic components and calculating a weighted mean of the monochromatic coefficients:⁹

$$\alpha'_{ij} = \frac{\sum_{\lambda} \Delta P_{i,\lambda} \alpha'_{ij,\lambda}}{P_i} \quad (3)$$

where the influence coefficients for a monochromatic excitation λ are given by

$$\alpha'_{ij,\lambda} = \frac{\mu_{j,\lambda} + A\mu_{j,\lambda_i}}{\mu_{i,\lambda} + A\mu_{i,\lambda_i}} - 1 \quad (4)$$

Finally, the values of the effective coefficients α_{ij} ,

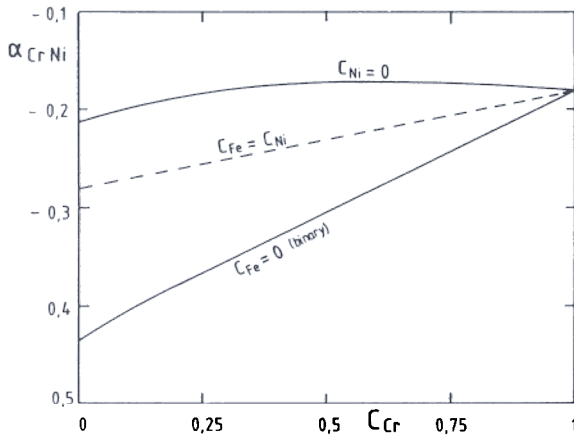


Figure 3. Chromium fluorescence in Cr-Fe-Ni system. Binary coefficient α_{CrNi} curve, limiting curve ($C_{Ni} \rightarrow 0$) and median curve ($C_{Fe} = C_{Ni}$). Rh target, 50-kV polychromatic excitation.

Table 3. Definitions of symbols

Symbol	Definition
ψ_1, ψ_2	Angle of incidence of primary radiation and angle of emergence of fluorescent radiation, respectively, measured from the specimen surface
$A = \frac{\sin \psi_1}{\sin \psi_2}$	Geometric factor
$q = \frac{\sin \psi_1}{\sin \psi_2} \frac{d\Omega}{4\pi}$	Collimation factor
C_i, C_j, C_k	Relative concentrations of elements i, j, k , etc.
I_λ	Spectral intensity distribution of primary radiation
λ	Wavelength of primary radiation
λ_0	Short wavelength limit of the continuous spectrum
$\lambda_{\text{abs},i}, \lambda_{\text{abs},j}$	Wavelengths of absorption edges of elements i, j , etc.
λ_i, λ_j	Wavelengths of fluorescent radiations of elements i, j , etc.
$\mu_{s,\lambda}$	Mass absorption coefficient of specimen s at wavelength λ
$\mu_{i,\lambda}, \mu_{j,\lambda}$	Mass absorption coefficients of elements i, j , etc., at wavelength λ
E_i, E_j	Excitation factors of elements i, j , etc., for a given spectral line. For example, E_i for the $K\alpha$ line is given by

$$E_i = \frac{r_K - 1}{r_K} \omega_K g_{K\alpha}$$

where $(r_K - 1)/r_K$ is the probability of K ionization by incident photons, ω_K the fluorescent yield and $g_{K\alpha}$ the probability of emission of a $K\alpha$ line in preference to other K lines

α'_{ik} , ..., are calculated by using Tertian's identities [Eqn (2)].

With these results we studied the theoretical variation of multi-component coefficients as a function of the composition.³⁴ Figure 3 shows the coefficients for the Cr-Fe-Ni system and the following three special cases: C_{Ni} close to 0% (limiting case), C_{Fe} equal to zero (binary case) and C_{Fe} equal to C_{Ni} (median case). The variations in Fig. 3 show that in the case of a multi-component system the binary coefficients are not precise enough, hence it is necessary to work with the effective coefficients corresponding to the composition.

THE ALGORITHM OF STANDARD COMPARISON

The method of effective coefficients, developed by Broll and Tertian,⁹ is based on a comparison algorithm to a standard. The effective coefficients α_{ij}^* , corresponding to a standard sample, are introduced into the Lachance-Trail equation for a standard:

$$C_i^* = R_i^* \left(1 + \sum_{j \neq i} \alpha_{ij}^* C_j^* \right)$$

The same coefficients α_{ij}^* are used for the unknown sample in the following equation:

$$C_i = R_i \left(1 + \sum_{j \neq i} \alpha_{ij}^* C_j \right)$$

By combining the two equations in order to eliminate the fluorescence intensity of the pure elements $I_{i,1}$, we obtain an algorithm of standard comparison:

$$C_i = C_i^* \frac{I_i}{I_i^*} \frac{\left(1 + \sum_{j \neq i} \alpha_{ij}^* C_j \right)}{\left(1 + \sum_{j \neq i} \alpha_{ij}^* C_j^* \right)} \quad (5)$$

We assume that in this algorithm the influence coefficients of the unknown sample are identical with those calculated for the standard ($\alpha_{ij} = \alpha_{ij}^*$). If the composition of the standard C_i^* and that of the unknown sample C_i are different, the composition obtained by Eqn (5) can be used as an approximate composition C_i^n , to calculate new effective α_{ij}^n which are reintroduced into the numerator of the algorithm of standard comparison allowing the calculation of a composition with a higher precision:

$$C_i^n = C_i^* \frac{I_i}{I_i^*} \frac{\left(1 + \sum_{j \neq i} \alpha_{ij}^n C_j \right)}{\left(1 + \sum_{j \neq i} \alpha_{ij}^* C_j^* \right)}$$

It must be emphasized, and this is very important, that even if the real conditions do not correspond completely to the hypothesis of the calculation or to the values of the fundamental parameters, this does not normally affect the accuracy of the analysis. The reason is that a small error in the coefficients is compensated by the use of two correction terms in the numerator and denominator. Several applications using the algorithm of standard comparison were presented by Broll.³⁶

APPLICATION OF THE ALGORITHM OF STANDARD COMPARISON TO SEVERAL STANDARD SAMPLES

The standard comparison algorithm requires a single standard of perfect quality and with exactly known concentrations. There also exists a variant which allows one to obtain the calibration with several standards. It uses the following algorithm:

$$C_i = a_i + b_i I_i \left(1 + \sum_{j \neq i} \alpha_{ij} C_j \right) \quad (7)$$

Now the effective coefficients α_{ij} are calculated according to several standards, either with a medium concentration for each element or with a typical concentration, i.e. the average of the highest and lowest concentrations. The influence coefficients of the trace elements on the major elements can be ignored.

The coefficients a_i and b_i are obtained by linear regression according to the following equation:

$$C_i = a_i + b_i I_i^{\text{corr}} \quad (8)$$

Table 4. Analysis of stainless-steel samples (%)

Alloy	Cr		Fe		Chem.	XRF
	Chem.	XRF	Chem.	XRF		
BAS 61	15.20	15.07	77.30	77.28	6.26	6.21
BAS 62	12.80	12.74	73.50	73.16	12.40	12.53
BAS 63	18.70	18.66	70.50	70.57	9.49	9.47
BAS 64	25.60	25.66	52.50	52.23	20.60	20.76
BAS 65	18.45	18.36	70.00	69.80	9.47	9.50
BAS 67	17.80	17.71	70.30	70.05	9.52	9.48
BAS 68	18.50	18.47	69.10	68.84	9.33	9.36

with

$$\begin{aligned} I_i^{\text{corr}} &= I_i \left(1 + \sum_{j \neq i} \alpha_{ij} C_j \right) \\ &= I_i (1 + M) \end{aligned} \quad (9)$$

M representing the matrix effects.

The solution of the equation system [Eqn (7)] gives approximate concentrations C_i^a of the unknown samples. The next step is the calculation of the coefficients α_{ij}^a based on the approximate composition of the unknown sample as well as the calculation of the coefficients α_{ij}^* for the standard whose concentrations are closest to the unknown. Alternatively, the closest standard can be taken individually for each element. Finally, the concentrations of the unknown sample are calculated with the standard comparison algorithm:

$$C_i = C_i^* \frac{I_i}{I_i^*} \frac{\left(1 + \sum_{j \neq i} \alpha_{ij}^a C_j \right)}{\left(1 + \sum_{j \neq i} \alpha_{ij}^* C_j^* \right)} \quad (10)$$

Table 4 gives the results obtained from eight BAS standards measured as unknowns.

Figures 4, 5 and 6 show for 28 Fe-based alloys with wide ranges of concentrations the measured fluorescence intensities and the intensities corrected for matrix effects [Eqn (9)] as a function of concentration of Cr, Fe and Ni, respectively, in the Cr-Fe-Ni system. The corrected intensities are higher than the measured intensities for iron, which has a high positive coefficient α_{FeCr} and a small negative coefficient α_{FeNi} . Nickel, which has positive coefficients α_{NiFe} and α_{NiCr} , shows the same effect. In contrast to Fe and Ni, for Cr the corrected

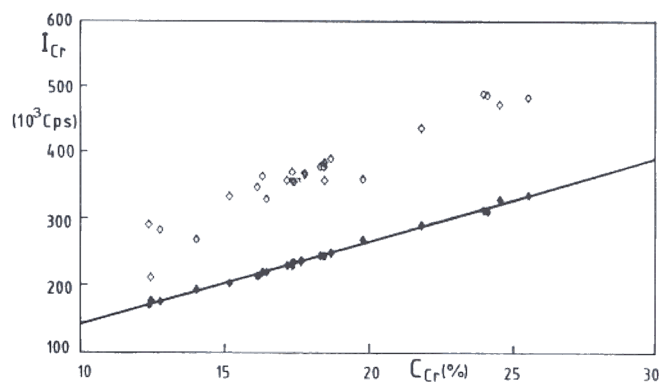


Figure 4. Calibration of chromium: (◇) without matrix correction; (◆) using effective coefficients.

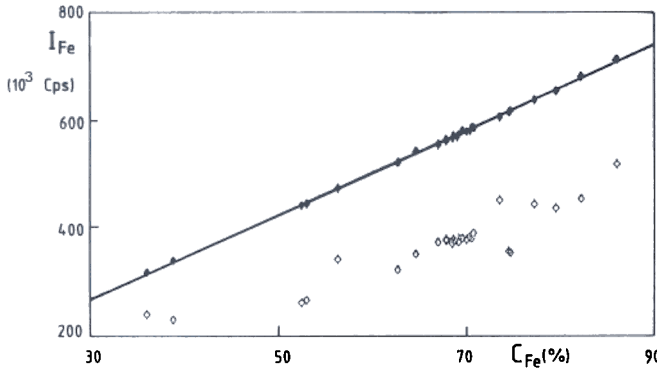


Figure 5. Calibration of iron: (◇) without matrix correction; (◆) using effective coefficients.

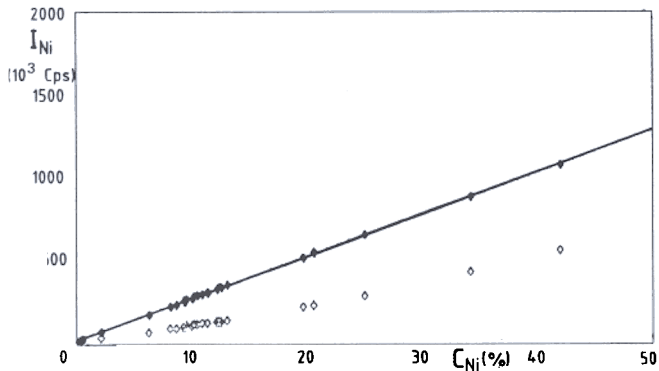


Figure 6. Calibration of nickel: (◇) without matrix correction; (◆) using effective coefficients.

intensities are lower than the measured intensities owing to negative coefficients α_{CrFe} and α_{CrNi} . The effective coefficients calculated with the typical concentrations are reported in Table 5.

APPLICATION TO MATERIALS WHERE A MAJOR ELEMENT IS NOT ANALYSED

In the analysis of stainless steel described above, the concentration of iron is often not exactly known in the standards and not determined by XRF analysis. Consequently, a major element k , which is not analysed, can be eliminated in the Lachance–Traill algorithm. Doing this, C_k is replaced with⁸

$$-\sum_{j \neq k} C_j = C_k$$

Table 5. Effective coefficients calculated for the stainless-steel samples

Element analysed	Interfering element		
	Cr	Fe	Ni
Cr	0	-0.48	-0.25
Fe	3.09	0	-0.44
Ni	1.40	1.96	0

Table 6. Modified effective coefficients used for the analysis of stainless-steel samples

Element analysed	Interfering element		
	Cr	Fe	Ni
Cr	0.28	0	0.07
Fe	0	0	0
Ni	-0.19	0	-0.66

which is introduced into the Lachance–Traill equation

$$\begin{aligned} C_i &= a_i + b_i I_i \left[+ \sum_{\substack{j \neq i \\ k \neq j}} \alpha_{ij} C_j + \alpha_{ik} C_k \right] \\ &= a_i + b_i I_i \left[+ \sum_{\substack{j \neq i \\ k \neq i}} \alpha_{ij} C_j + \alpha_{ik} - \sum_{j \neq k} \alpha_{ik} C_j \right] \\ &= a_i + b_i (1 + \alpha_{ik}) I_i \left[+ \sum_{j \neq k} \left(\frac{\alpha_{ij} - \alpha_{ik}}{1 + \alpha_{ik}} \right) C_j \right] \end{aligned}$$

with $\alpha_{ii} = 0$ for $j = i$. The expression can be rewritten as

$$C_i = a_i + b'_i I_i \left(1 + \sum_{j \neq k} \alpha'_{ij} C_j \right) \tag{11}$$

where

$$b'_i = b_i (1 + \alpha_{ik})$$

$$\alpha'_{ij} = \frac{\alpha_{ij} - \alpha_{ik}}{1 + \alpha_{ik}}$$

$$\alpha'_{ii} = \frac{-\alpha_{ik}}{1 + \alpha_{ik}}$$

Using this approach, the element k is eliminated from the algorithm (7). The modified coefficients α'_{ii} , α'_{ij} are now obtained, whereas the α'_{ik} , α'_{jk} (and also the α_{ki} , α_{kj}) disappear.

Table 6 shows the modified effective coefficients which were calculated for the same composition as that used for the calculation of the original coefficients given in Table 5. Table 7 reports the concentrations of the unknown samples obtained with modified effective coefficients, iron not being analysed. The results are less precise, especially for Cr. As a rule, the best results are obtained by including all major elements in the correction procedure [e.g. Eqn (7)].

Table 7. Analysis of stainless-steel samples without measurement of iron (%)

Alloy	Cr			
	Chem.	XRF	Chem.	XRF
BAS 61	15.20	15.95	6.26	6.30
BAS 62	12.80	13.54	12.40	12.56
BAS 63	18.70	18.96	9.49	9.54
BAS 64	25.60	24.11	20.60	20.69
BAS 65	18.45	18.57	9.47	9.55
BAS 67	17.80	17.96	9.52	9.54
BAS 68	18.50	18.64	9.33	9.42

TRACE ELEMENT ANALYSIS. TRACE MODEL

Differentiating the Lachance–Traill algorithm yields

$$\frac{\partial C_i/C_i}{\partial C_j} = \frac{\alpha_{ij}}{1 + \sum_{j \neq i} \alpha_{ik} C_j}$$

This relationship shows that a small variation of the concentration C_j with the coefficient α_{ij} being close to -1 leads to a considerable change in the concentration C_i .

Coefficients close to -1 are obtained in the case of a heavy element being present in a light matrix (e.g. the determination of Sr in geological materials). To reduce this influence, we introduce the equation

$$\sum_{j \neq i} C_j + C_i = 1$$

in the Lachance–Traill algorithm. The algorithm can be written as

$$C_i = a_i + b_i I_i \left[C_i + \sum_{j \neq i} (1 + \alpha_{ij}) C_j \right]$$

and is transformed to

$$C_i = a'_i + b'_i I_i \sum_{j \neq i} (1 + \alpha_{ij}) C_j \quad (12)$$

where

$$a'_i = \frac{a_i}{1 - b_i I_i}$$

and

$$b'_i = \frac{b_i}{1 - b_i I_i}$$

Equation (12) is called the trace model. The differential of this model:

$$\frac{\partial C_i/C_i}{\partial C_j} = \frac{1 + \alpha_{ij}}{\sum_{j \neq i} (1 + \alpha_{ik}) C_j}$$

shows that a variation of the concentration C_j with the coefficient α_{ij} (close to -1) now has less influence on the concentration C_i .

Table 8 shows the analytical results obtained for the analysis of Sr in various geological standards prepared as pressed pellets without binder. A striking improvement using the trace model instead of the Lachance–Traill model is obtained.

COMPARISON WITH THE INTENSITY MODEL

From a set of seven plant materials with known concentrations, four samples were used as standards (potatoes, spinach, tomato leaves and pine needles) and three as 'unknowns' to check the calibration.

Typical plant materials have the following composition: Ca, K and Cl 0–5%, S, P, Si, Al, Mg and Na 0–2% and Zn, Cu, Fe and Mn as traces. The remainder of the

Table 8. Analysis of strontium in geological samples (ppm)

Standard	Chem.	Lachance–Traill		Trace model	
		XRF	Dev.*	XRF	Dev.
GSR-1	106	104	-2	108	2
RGM-1	100	96	-4	102	2
GM	133	125	-8	132	-1
NIM-G	10	10	0	10	0
GH	10	9	-1	9	-1
JG-2	16	15	-1	16	0
BE-N	1370	1419	49	1393	23
NIM-D	3	2	-1	2	-1
JGB-1	321	309	-12	336	15
NBS 688	169	151	-18	172	3
STM-1	700	685	-15	687	-13
SY-2	275	257	-18	270	-5
GSR-2	790	927	137	799	9
NIM-S	62	59	-3	64	2
GS-N	570	556	-14	563	-7
QLO-1	350	302	-48	330	-20
MA-N	84	98	14	81	-3
GA	310	281	-29	289	-21
JG-1A	185	171	-14	180	-5
BM	228	248	20	226	-2
BHVO-1	420	347	-73	394	-26

* Dev. = absolute deviation.

light matrix is considered to be carbon, which is not analysed, hence the algorithm in Eqn (11) is applied. For the minor elements we also used the intensity model with multiple regression corresponding to the equation

$$C_i = a_i + b_i I_i \left(1 + \sum_{j \neq i} \alpha_{ij} I_j \right) \quad (13)$$

Table 9 shows the analytical results for phosphorus and potassium. Again, the superiority of the effective coefficient method over the multiple regression method is demonstrated.

With the regression method, the result of the analysis of potassium is completely wrong in the unknown 'silage', where not every element is in the concentration ranges of the standards used. In contrast, the effective coefficient method matches the matrix effects more correctly.

Table 9. Analysis of plants (%)^a

Plants	Phosphorus			Potassium		
	Chem.	FCM	MR	Chem.	FCM	MR
Standards						
Potatoes	0.18	0.216	0.242	1.88	1.71	1.93
Spinach	0.55	0.531	0.512	3.56	3.74	3.64
Tomato leaves	0.34	0.349	0.346	4.46	4.43	4.43
Pine needles	0.19	0.185	0.202	1.56	1.36	1.37
Unknowns						
Epicea	0.17	0.165	0.187	0.61	0.52	0.59
230-31	0.15	0.153	0.175	0.32	0.32	0.37
Silage	0.43	0.432	0.430	3.68	3.66	5.00

^a FCM = fundamental coefficient method; MR = multiple regression.

For trace element analysis the concentrations were corrected according to the equation

$$C_i = a_i + b_i \frac{I_i}{I_C} \quad (14)$$

where the intensity I_C of the Compton radiation of Rh $K\alpha$ is used as the internal standard.

In the case of the trace elements Zn and Cu we also note a remarkable improvement in the results given in Table 10 obtained using the effective coefficient method.

CONCLUSION

The superiority of the effective coefficient method has been demonstrated in various applications. It has been applied to the analysis of major elements requiring maximum precision and for trace element analysis in various materials.

The possibilities of further development of this method depend largely on a better knowledge of the fundamental parameters and the possibility of including two additional physical effects; the first is tertiary fluo-

Table 10. Analysis of trace elements in plants (ppm)^a

Plants	Zinc			Copper		
	Chem.	FCM	CC	Chem.	FCM	CC
Standards						
Potatoes	17.0	14.0	16.9	3.2	2.9	7.1
Spinach	50.0	49.5	49.8	12.0	10.7	8.5
Tomato leaves	62.0	64.2	62.5	11.0	12.0	8.8
Pine needles	160.0	159.5	159.9	4.2	4.8	7.2
Unknowns						
Epicea	34.4	28.1	54.4	3.1	2.5	10.3
230-31	20.3	17.5	24.2	1.4	1.9	7.3
Silage	52.5	51.8	48.3	8.0	7.7	7.7

^a FCM = fundamental coefficient method; CC = Compton correction.

rescence,^{38,39} which, in the most unfavourable cases, can account for as much as 5% of the total fluorescence intensity, and the second is the contribution of scattering,^{40,41} which can enhance the measured intensity considerably, particularly in the case of samples with a very light matrix.

REFERENCES

- J. W. Criss and L. S. Birks, *Anal. Chem.* **40**, 1080 (1968).
- J. W. Criss, L. S. Birks and J. V. Gilfrich, *Anal. Chem.* **50**, 33 (1978).
- J. W. Criss, *Adv. X-Ray Anal.* **23**, 93 (1980).
- G. Y. Tao, P. A. Pella and R. M. Rousseau, *NBSGSC—A Fortran Program for Quantitative X-Ray Spectrometric Analysis Using X-Ray Tube Excitation*. NBS Technical Note No. 1213, National Bureau of Standards, Washington, DC (1985).
- G. R. Lachance and R. J. Traill, *Can. Spectrosc.* **11**, 43 (1968).
- F. Claisse and M. Quintin, *Can. Spectrosc.* **12**, 129 (1967).
- G. R. Lachance, paper presented at the International Conference on Industrial Inorganic Elemental Analysis, Metz, France, June 1981, paper No. 47.
- W. K. De Jongh, *X-Ray Spectrom.* **2**, 151 (1973).
- N. Broll and R. Tertian, *X-Ray Spectrom.* **12**, 30 (1983).
- R. Tertian, 4ème Colloque International sur les Méthodes Analytiques par Rayonnements X, Strasbourg, Preprint 113 (1977).
- R. Rousseau, *X-Ray Spectrom.* **13**, 121 (1984).
- R. Rousseau, *X-Ray Spectrom.* **13**, 115 (1984).
- L. Gerward, *X-Ray Spectrom.* **15**, 29 (1986).
- B. A. R. Vrebos and P. A. Pella, *X-Ray Spectrom.* **17**, 3 (1988).
- J. Leroux and T. P. Thinh, *Revised Tables of X-Ray Mass Attenuation Coefficients*. Claisse Scientific Corporation, Quebec (1977).
- J. L. Campbell and D. DeForge, *X-Ray Spectrom.* **18**, 235 (1989).
- W. Hanke, J. Wernisch and C. Poehn, *X-Ray Spectrom.* **14**, 43 (1985).
- C. Poehn, J. Wernisch and W. Hanke, *X-Ray Spectrom.* **15**, 120 (1985).
- C. Bhan, S. N. Chaturvedi and N. Nath, *X-Ray Spectrom.* **15**, 217 (1986).
- S. Kumar, S. Singh, D. Mehta, N. Singh, P. C. Mangal and P. N. Trehan, *X-Ray Spectrom.* **16**, 203 (1987).
- H. S. Sahota, R. Singh and N. P. S. Sidhu, *X-Ray Spectrom.* **17**, 99 (1988).
- K. L. Williams, *An Introduction to X-Ray Spectrometry*. Allen and Unwin, London (1987).
- D. B. Brown and J. V. Gilfrich, *J. Appl. Phys.* **42**, 4044 (1971).
- D. B. Brown, J. V. Gilfrich and M. C. Peckerar, *J. Appl. Phys.* **46**, 4537 (1975).
- T. C. Loomis and H. D. Keith, *X-Ray Spectrom.* **5**, 104 (1976).
- M. Murata and H. Shibahara, *X-Ray Spectrom.* **10**, 41 (1981).
- S. Planitz-Penno, U. Schulte and G. Stork, *Fresenius' Z. Anal. Chem.* **312**, 600 (1982).
- M. G. Brunetto and J. A. Riveros, *X-Ray Spectrom.* **13**, 60 (1984).
- R. Tertian and N. Broll, *X-Ray Spectrom.* **13**, 134 (1984).
- P. A. Pella, L.-Y. Feng and J. A. Small, *X-Ray Spectrom.* **14**, 125 (1985).
- A. Markowicz, H. Storms and R. Van Grieken, *X-Ray Spectrom.* **15**, 131 (1986).
- H. Ebel, M. F. Ebel, J. Wernisch, C. Poehn and H. Wiederschwinger, *X-Ray Spectrom.* **18**, 89 (1989).
- R. Tertian and F. Claisse, *Principles of Quantitative X-Ray Fluorescence Analysis*. Heyden, London (1982).
- N. Broll, PhD Thesis, Strasbourg (1985).
- F. Spagnoli, Diplomarbeit, University of Karlsruhe (1984).
- N. Broll, *X-Ray Spectrom.* **15**, 271 (1986).
- N. Broll, *X-Ray Spectrom.* **19**, 193 (1989).
- T. Shiraiwa and N. Fujino, *Jpn. J. Appl. Phys.* **5**, 886 (1966).
- G. Pollai and H. Ebel, *Spectrochim. Acta, Part B* **26**, 761 (1971).
- G. Pollai, M. Mantler and H. Ebel, *Spectrochim. Acta, Part B* **26**, 733 (1971).
- H. D. Keith and T. C. Loomis, *X-Ray Spectrom.* **7**, 225 (1978).